Supporting Information

Emergence of Solvent-Separated Na^+-Cl^- Ion Pair in Salt Water: Photoelectron Spectroscopy and Theoretical Calculations

Gao-Lei Hou,[1] Cheng-Wen Liu,[2] Ren-Zhong Li,[1] Hong-Guang Xu,[1,3] Yi Qin Gao,[2]* Wei-Jun Zheng[1,3]*

[1] *Beijing National Laboratory for Molecular Sciences, State Key Laboratory of Molecular Reaction Dynamics, Institute of Chemistry, Chinese Academy of Sciences, Beijing 100190, China*

[2] *Beijing National Laboratory for Molecular Sciences, Institute of Theoretical and Computational Chemistry, College of Chemistry and Molecular Engineering, Peking University, Beijing 100871, China*

[3] *University of Chinese Academy of Sciences, Beijing 100049, China*

* e-mail: zhengwj@iccas.ac.cn, gaoyq@pku.edu.cn

Table of Contents

1. Experimental and Theoretical Methods

Experimental methods. The experiments were conducted on a home-built apparatus consisting of a time-of-flight (TOF) mass spectrometer and a magnetic-bottle photoelectron spectrometer.[S1] Briefly, the $NaCl^-(H_2O)_n$ clusters were produced in a laser vaporization source, in which a rotating and translating NaCl disk target was ablated by the second harmonic (532 nm) light pulses from a nanosecond Nd:YAG laser, while helium carrier gas with ~4 atm backing pressure seeded with water vapor was allowed to expand through a pulsed valve to generate the hydrated $NaCl^-$ clusters and to cool these clusters. The cluster anions were mass-analyzed by the TOF mass spectrometer. The $NaCl^-(H_2O)_n$ (n = 0-6) clusters were each mass-selected and decelerated before being photodetached by the 1064 and/or 532 nm photons from another nanosecond Nd:YAG laser. The photodetached electrons were energy-analyzed by the magnetic-bottle photoelectron spectrometer. The photoelectron spectra were calibrated with the spectra of Cs^- and Bi^- taken at similar conditions. The instrumental resolution was approximately 40 meV for electrons with 1 eV kinetic energy. The ADE was determined from the onset of each peak by drawing a straight line along the leading edge of that peak across the spectrum baseline and was given by adding the instrumental resolution to account for the spectral broadening due to instrumental resolution. The VDE was obtained from the maximum of each peak.

Theoretical methods. We utilized the integrated tempering sampling (ITS) molecular dynamics[S2] to generate ensembles of structures of $NaCl(H_2O)_n$ clusters with low configuration energies, which allows us to get more complete sets of low-lying structures. The low-energy structures obtained from the ITS calculations were first optimized using classical force field. The structures of $NaCl^{-/0}(H_2O)_n$ clusters were then fully optimized further with density functional theory (DFT) employing the long-range corrected hybrid functional LC-ωPBE[S3] as implemented in the Gaussian 09 program package.[S4] The Pople's all-electron basis set 6-311++G(d, p)[S5] was used for all the atoms. Harmonic vibrational frequencies were calculated to make sure that the optimized structures are the real local minima. The $NaCl^{-/0}(H_2O)_n$ clusters have many low-lying isomers which are close in energy and the orders of their relative stabilities may vary at different levels of

theory. Thus, it is very important to obtain more accurate relative energies of those isomers with high level theoretical methods. In this work, in order to get more accurate energetic information, single-point energy calculations were also performed using the CCSD(T)[S6] and MP2[S7] methods with very large basis sets, such as aug-cc-pVTZ[S8, S9] and maug-cc-pVTZ[S10] basis sets. The theoretical vertical detachment energies (VDEs) were calculated as the energy differences between the neutrals and the anions both at the anionic geometries. The theoretical adiabatic detachment energies (ADEs) were calculated as the energy differences between the neutrals and the anions with the neutrals relaxed to the nearest local minima using the geometries of the anions as initial structures. All the relative energies and theoretical ADEs have been corrected by the zero-point vibrational energies (ZPE) obtained at the LC-ωPBE/6-311++G(d, p) level of theory.

2. Molecular Dynamics Simulation Details

The well-established enhanced sampling MD simulations–the Integrated Tempering Sampling (ITS),[S2,S11] were performed for the large $NaCl(H_2O)_n$ (n = 7, 8, 9, 10, and 12) clusters. Briefly, in the ITS simulation, a modified potential energy is obtained from a summation of Boltzmann factors over a series of temperatures, thus the sampled potential energy range is largely expanded. In this study, we used 300 discrete temperatures in the range of 70-270 K. The three-point-charge SPC/E[S12] model for water molecules and the popular ion parameters, ions08,[S13] for Na^+ and Cl^- ions were utilized. All the simulations employed an integral time step of 0.5 fs. The temperatures were maintained at 200 K during the simulations, by using Langevin dynamics[S14] with a collision frequency of 1 ps^{-1}. All the simulations were performed in vacuum using a non-periodic boundary condition where the non-bonded interactions are only Lennard-Jones and Coulomb interactions. To assure the intra-cluster interactions to be fully calculated, non-bonding interaction cutoffs used in simulations was 15 Å. All the simulations were conducted with the SANDER module of AMBER9.0 software package.[S15]

To obtain the thermodynamic properties of the clusters, we run MD simulation with the biased potential function U′(r) = U+f(U) at equilibrium in the ITS simulation.[S16] This will yield a distribution function over the configuration space,

$$\rho'(\mathrm{r}) = e^{-\beta \mathrm{U}'(\mathrm{r})}/Q' \tag{1}$$

where $\beta = 1/\mathrm{k}_B T$, k_B being the Boltzmann constant, T being the temperature, and $Q' = \int e^{-\beta \mathrm{U}'(\mathrm{r})} dr$. In the simulation, U′(r) is a known function of U(r), thus the distribution function with original (unbiased) potential $\rho(\mathrm{r})$ can be recovered from $\rho'(\mathrm{r})$ as:

$$\rho(\mathrm{r}) = \frac{e^{-\beta \mathrm{U}(\mathrm{r})}}{Q} = e^{-\beta \mathrm{U}'(\mathrm{r})} \times \frac{e^{-\beta[\mathrm{U}(\mathrm{r})-\mathrm{U}'(\mathrm{r})]}}{Q} = \rho'(\mathrm{r}) \frac{e^{-\beta[\mathrm{U}(\mathrm{r})-\mathrm{U}'(\mathrm{r})]} Q'}{Q} \tag{2}$$

where $Q = \int e^{-\beta \mathrm{U}(\mathrm{r})} dr$.

3. Population Analyses of the CIP and SSIP Structures in $NaCl(H_2O)_n$ (n = 8, 9, 10, and 12) Clusters

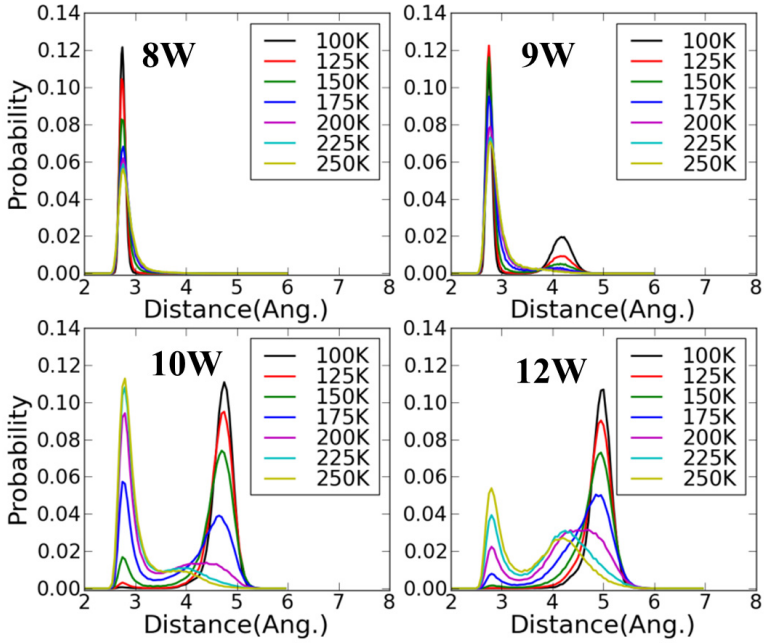

Figure S1. The Na–Cl distance distribution of different clusters at a series of selected temperatures obtained from ITS simulation trajectories.

Figure S1 presents the distribution functions of Na–Cl distance as a function of temperature obtained from the ITS simulation trajectories. It can be seen that the Na–Cl distance in $NaCl(H_2O)_8$ remains constant (about 2.8 Å, corresponding to CIP) in the temperature range of 100-250 K. Two features with the Na–Cl distance being ~2.8 (CIP) and ~4.2 Å (SSIP) were observed for $NaCl(H_2O)_9$ at 100 K. However, when the temperature increases from 100 to 250 K, the SSIP features gradually disappears, indicating that the SSIP structures are not stable compared to the CIP structures at high temperature. For n = 10, there is nearly no CIP features at 100 K, and the Na–Cl distance for the SSIP features increases to ~4.8 Å. As the temperature increases, the probability of the SSIP features decreases while that of the CIP features increases. However, there is still population of SSIP features even at 250 K, except that the features become broader and shift slightly to the shorter Na–Cl distance. For $NaCl(H_2O)_{12}$, the SSIP features are much more prominent over the CIP features at the temperature range of 100-200 K, and the populations of the two features become comparable at 250 K. Besides, the SSIP features become

broader and shift slightly to the shorter Na–Cl distance at higher temperature, similar as for $NaCl(H_2O)_{10}$. Overall, it can be seen that the results from the MD simulations at low temperature are in good agreement with those from the quantum chemical calculations; while at high temperature, the simulations show that the probability of the SSIP feature becomes smaller and that of the CIP feature becomes larger, thus showing a strong temperature-dependent fashion especially for the clusters with 10 and 12 water molecules.

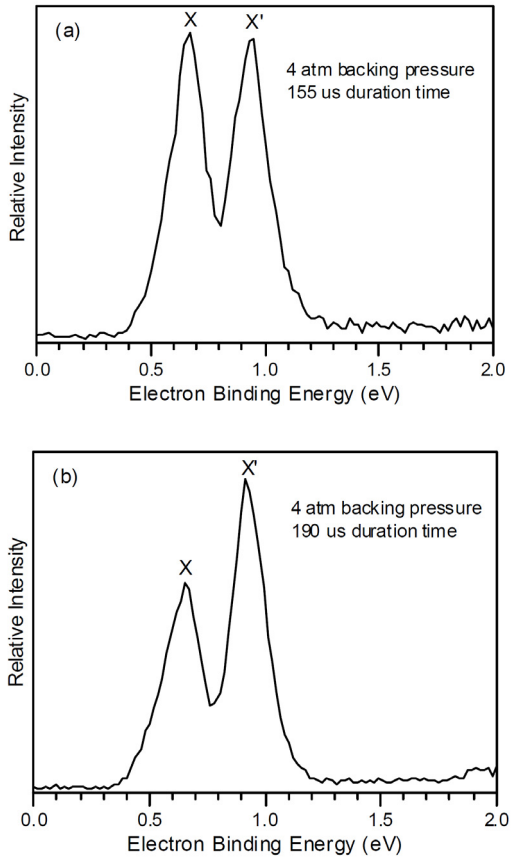

Figure S2. Photoelectron spectra of $NaCl^{-}(H_2O)$ measured with 532 nm photons at different experimental conditions. The change of the relative intensities of X and X′ features shown in (a) and (b) clearly indicates they come from different isomers.

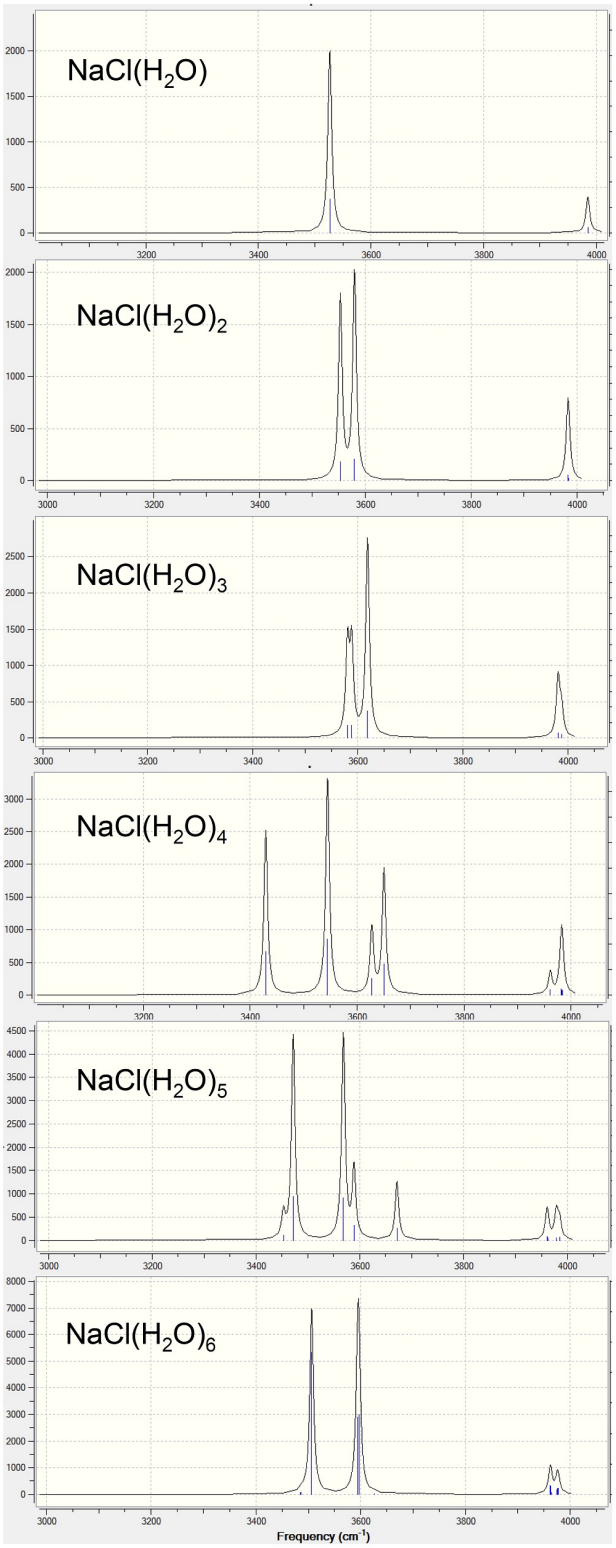

Figure S3. Simulated infrared spectra of the most stable structures of NaCl $(H_2O)_n$ (n = 1-6) in the O–H stretch vibrational range.

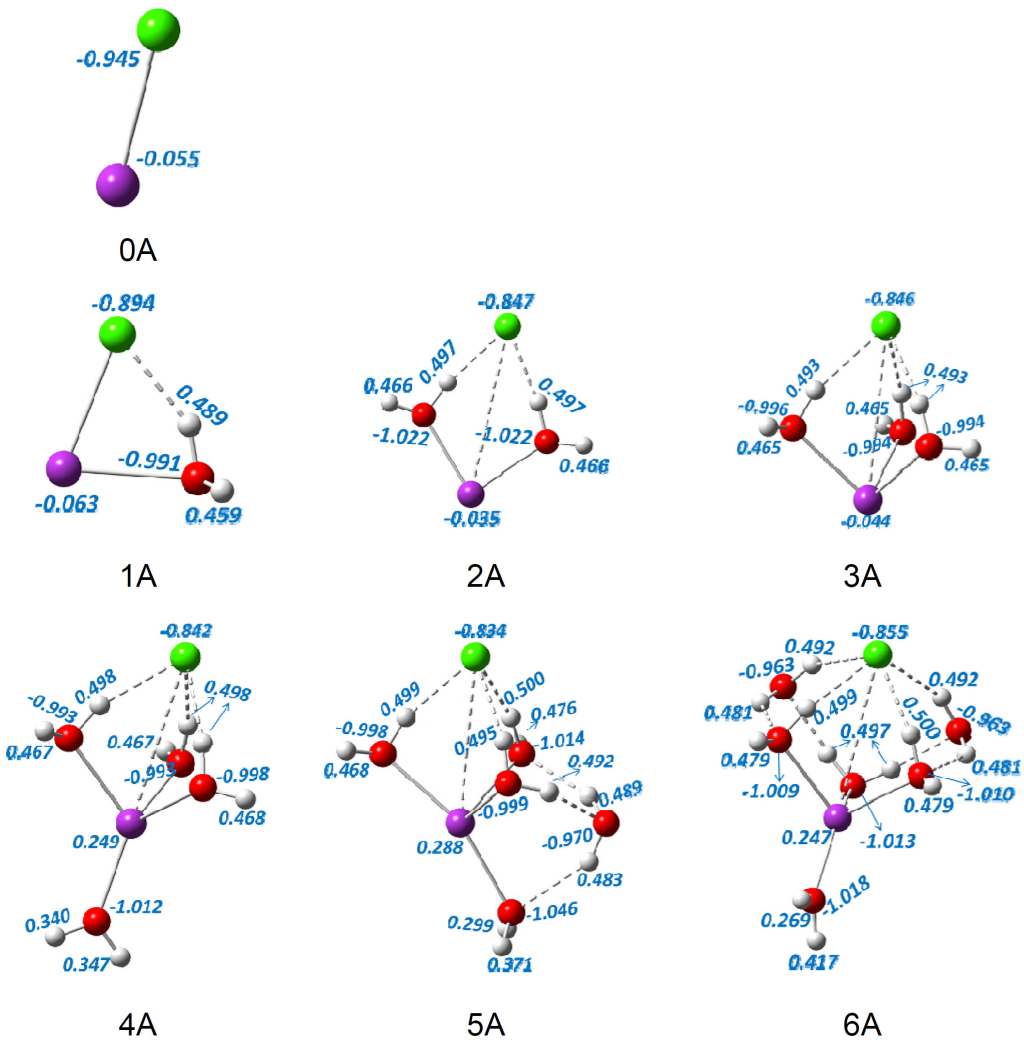

Figure S4. Natural population charge distributions of the most stable structures of the $NaCl^{-}(H_2O)_n$ (n = 0-6) clusters.

1

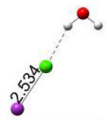

0.00 [0.93]

0.02 [0.53]

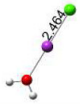

0.05 [0.66]

2

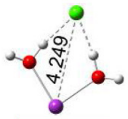

0.00 [0.73]

0.05 [0.40]

0.07 [0.49]

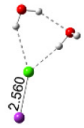

0.09 [1.09]

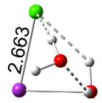

0.11 [0.61]

0.16 [0.77]

3

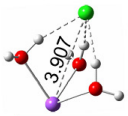

0.00 [0.37]

0.03 [0.45]

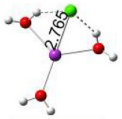

0.06 [0.40]

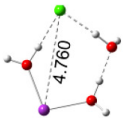

0.09 [0.77]

0.10 [0.47]

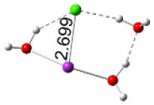

0.10 [0.24]

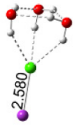

0.11 [1.21]

0.12 [0.38]

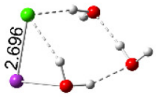

0.15 [0.58]

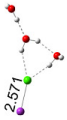

0.17 [1.19]

0.17 [0.59]

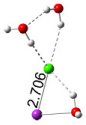

0.20 [0.85]

0.25 [0.87]

4

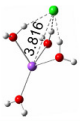

0.00 [0.43]

0.09 [0.31]

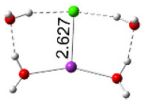

0.11 [0.16]

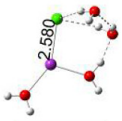

0.11 [0.50]

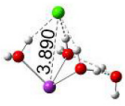

0.14 [0.56]

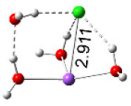

0.15 [0.15]

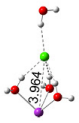

0.15 [0.51]

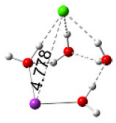

0.16 [0.94]

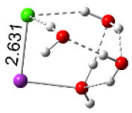

0.18 [0.70]

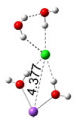

0.20 [0.97]

0.20 [0.53]

0.20 [0.74]

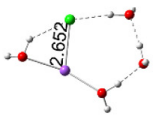

0.21 [0.16]

0.21 [0.25]

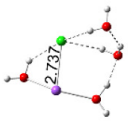

0.21 [0.24]

0.22 [0.48]

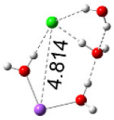

0.22 [0.93]

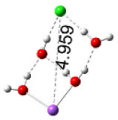

0.22 [0.90]

0.23 [0.66]

0.23 [0.17]

0.23 [0.71]

0.24 [1.37]

0.24 [0.96]

0.27 [0.41]

0.28 [0.94]

0.28 [0.52]

0.30 [0.76]

0.30 [0.92]

0.31 [0.29]

0.31 [1.31]

0.32 [1.07]

0.33 [0.62]

0.34 [1.15]

5

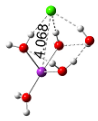

0.00 [0.37]

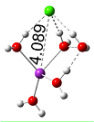

0.02 [0.44]

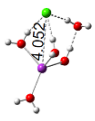

0.03 [0.49]

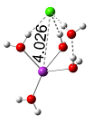

0.04 [0.39]

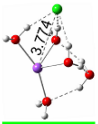

0.06 [0.64]

0.06 [0.24]

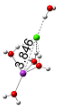

0.09 [0.46]

0.10 [0.60]

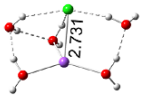

0.10 [0.23]

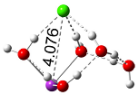

0.12 [0.76]

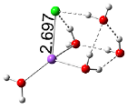

0.12 [0.33]

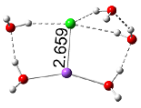

0.13 [0.34]

0.13 [0.30]

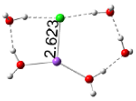

0.13 [0.13]

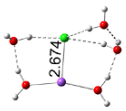

0.16 [0.16]

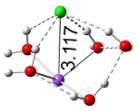

0.16 [0.26]

0.17 [0.43]

0.17 [1.63]

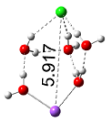

0.17 [0.87]

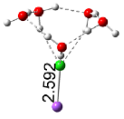

0.18 [1.49]

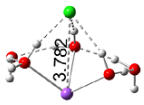

0.18 [0.86]

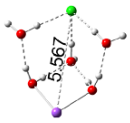

0.19 [0.74]

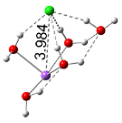

0.20 [0.35]

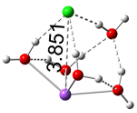

0.21 [0.17]

0.21 [0.80]

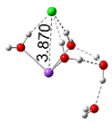

0.21 [0.97]

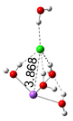

0.21 [0.58]

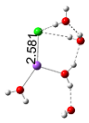

0.22 [0.73]

0.22 [0.44]

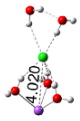

0.23 [0.71]

0.23 [0.70]

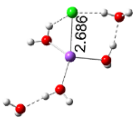

0.24 [0.28]

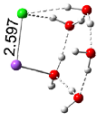

0.25 [1.06]

0.27 [1.68]

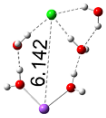

0.28 [1.20]

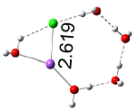

0.29 [0.21]

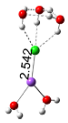

0.30 [1.06]

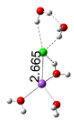

0.30 [0.83]

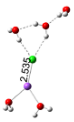

0.35 [1.07]

0.38 [1.14]

0.46 [1.43]

6

0.00 [0.57]

0.03 [0.43]

0.04 [0.02]

0.06 [0.67]

0.06 [0.68]

0.07 [0.68]

0.07 [0.30]

0.08 [0.36]

0.08 [0.80]

0.08 [0.22]

0.09 [0.85]

0.09 [0.21]

0.09 [0.47]

0.09 [0.68]

0.09 [0.52]

0.10 [0.41]

0.10 [0.70]

0.10 [0.11]

0.10 [0.62]

0.11 [0.49]

0.12 [0.58]

0.12 [0.58]

0.13 [0.75]

0.13 [0.13]

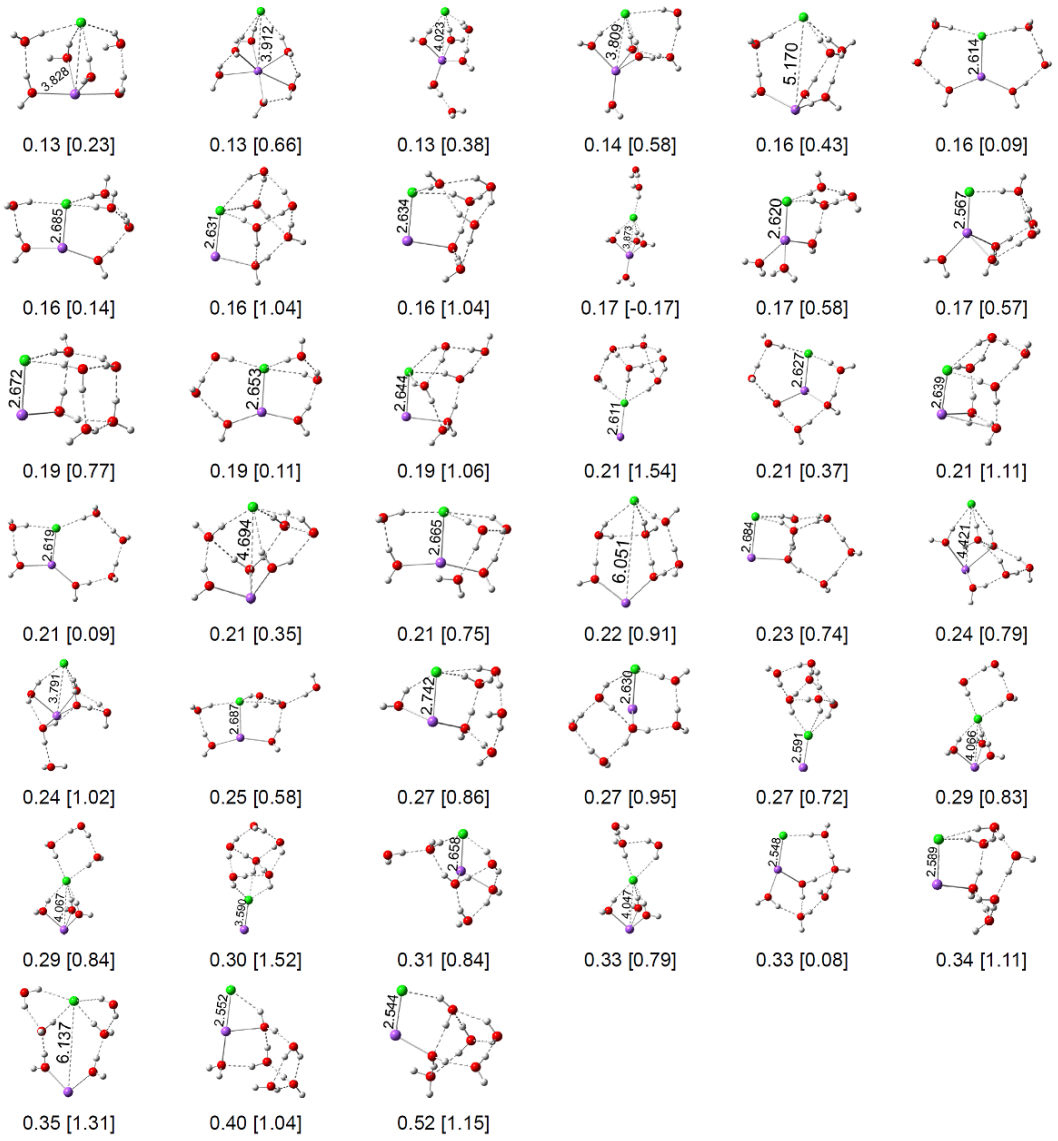

Figure S5. Complete list of optimized isomers of $NaCl^{-}(H_2O)_n$ (n = 1−6) at LC-ωPBE/6-311++G(d,p) level. Those reported in the main text are highlighted in green. Relative energies (in eV using LC-ωPBE functional within ZPE correction), theoretical VDEs (in eV, in brackets) and Na–Cl distances (in Å) are indicated.

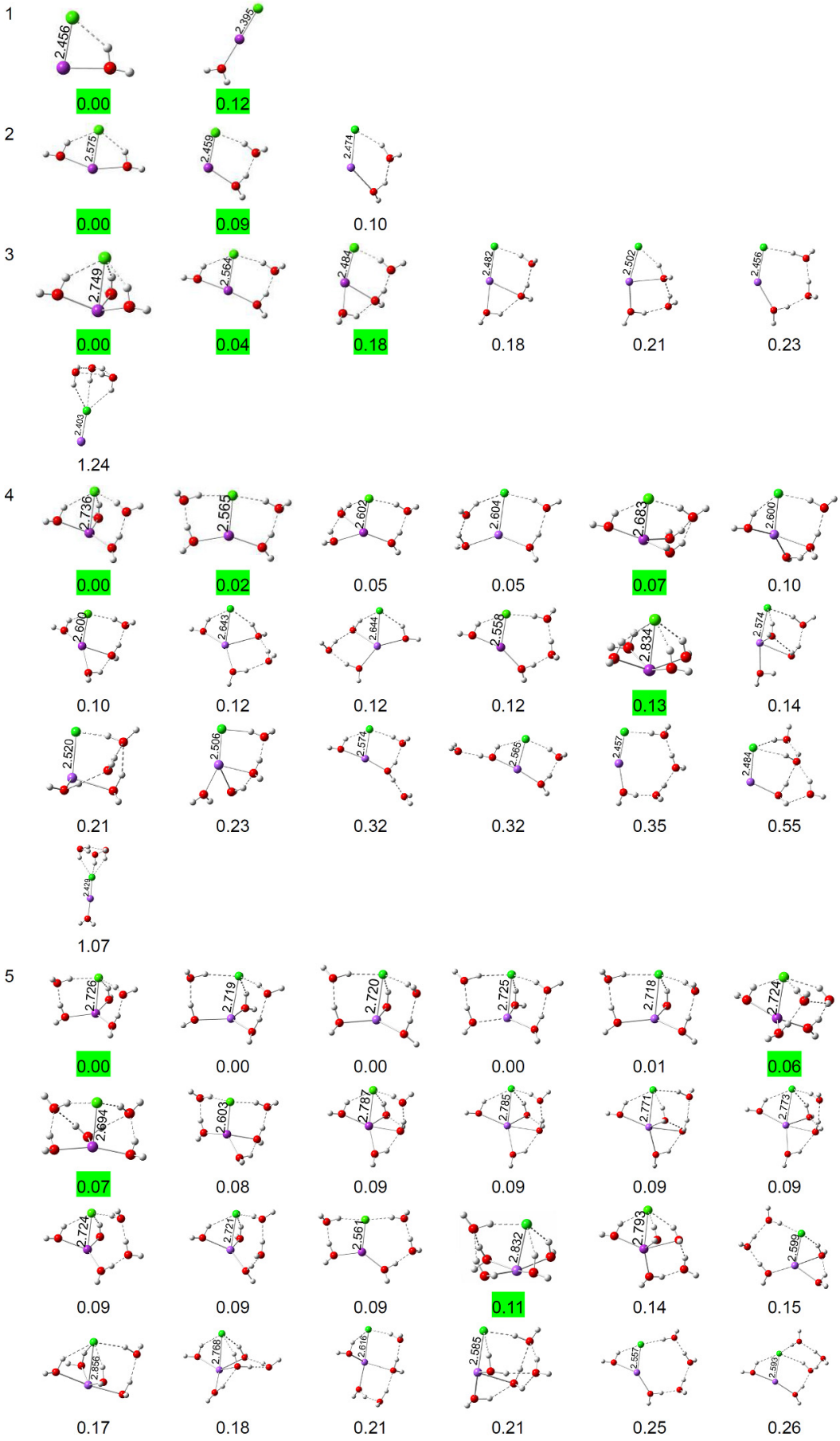
1
2.456
0.00
2.395
0.12
2
2.575
0.00
2.459
0.09
2.474
0.10
3
2.749
0.00
2.564
0.04
2.484
0.18
2.482
0.18
2.502
0.21
2.456
0.23
2.403
1.24
4
2.736
0.00
2.565
0.02
2.602
0.05
2.604
0.05
2.683
0.07
2.600
0.10
2.600
0.10
2.643
0.12
2.644
0.12
2.558
0.12
2.834
0.13
2.574
0.14
2.520
0.21
2.506
0.23
2.574
0.32
2.566
0.32
2.457
0.35
2.484
0.55
2.493
1.07
5
2.726
0.00
2.719
0.00
2.720
0.00
2.725
0.00
2.718
0.01
2.724
0.06
2.694
0.07
2.603
0.08
2.787
0.09
2.785
0.09
2.771
0.09
2.773
0.09
2.724
0.09
2.721
0.09
2.561
0.09
2.832
0.11
2.793
0.14
2.599
0.15
2.856
0.17
2.768
0.18
2.616
0.21
2.585
0.21
2.557
0.25
2.593
0.26

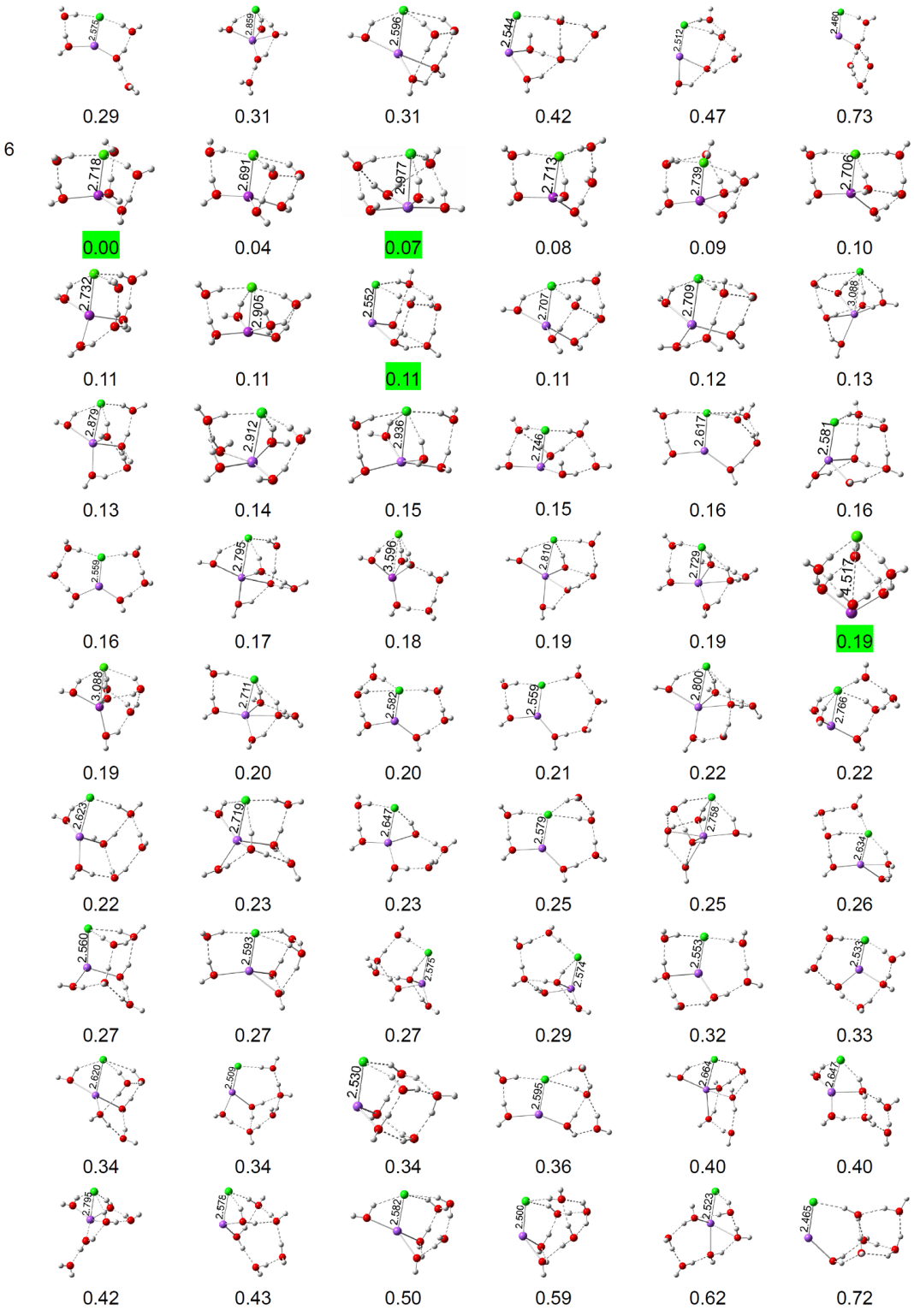

Figure S6. Complete list of optimized isomers of $NaCl(H_2O)_n$ (n = 1−6) at LC-ωPBE/6-311++G(d,p) level. Those reported in the main text are highlighted in green. Relative energies (in eV using LC-ωPBE functional within ZPE correction) and Na–Cl distances (in Å) are indicated.

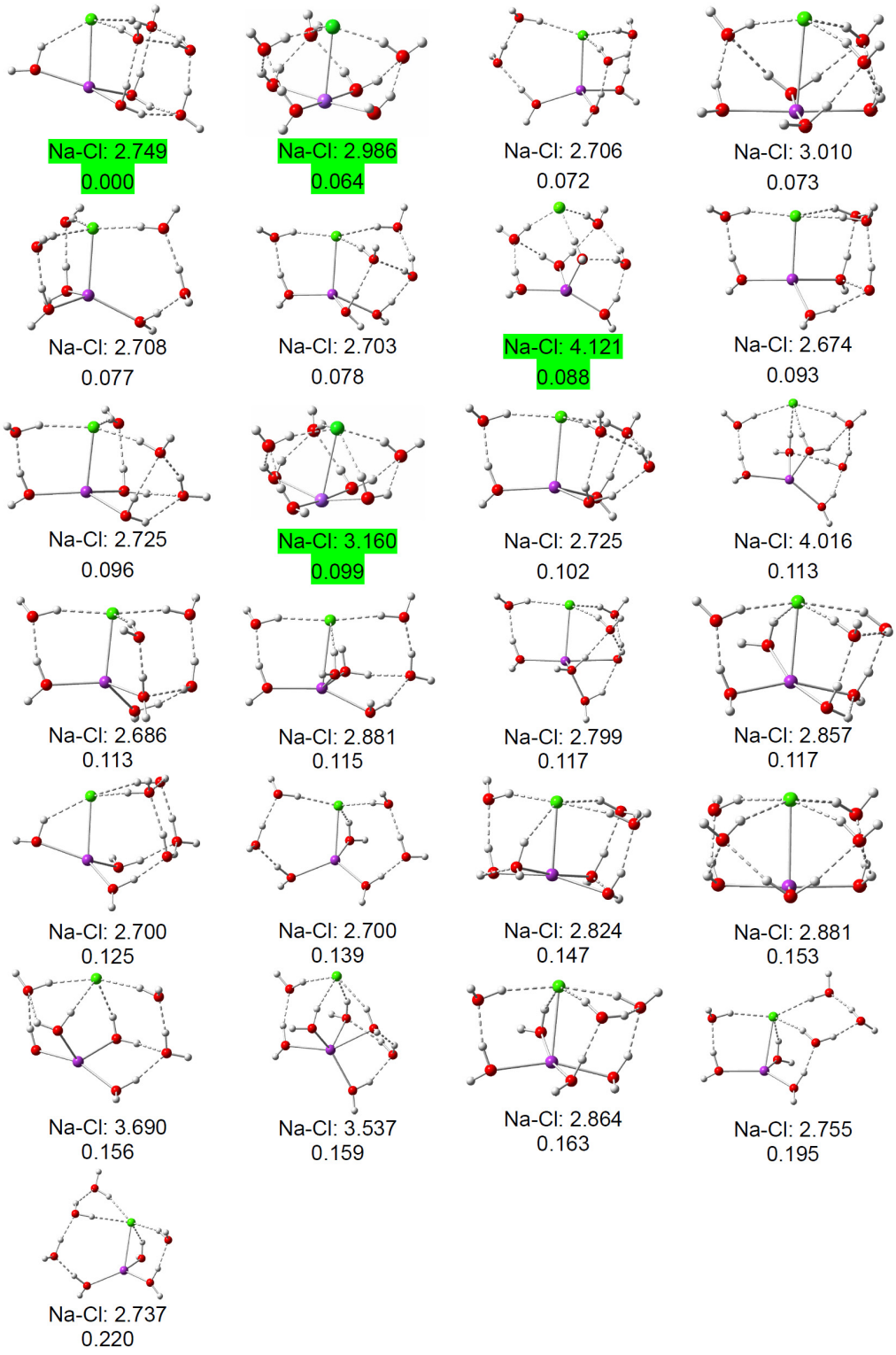

Figure S7. Complete list of optimized isomers of $NaCl(H_2O)_7$ at LC-ωPBE/6-311++G(d,p) level. Those reported in the main text are highlighted in green. Relative energies (in eV using LC-ωPBE functional within ZPE correction) and Na–Cl distances (in Å) are indicated.

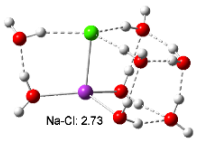

0.000

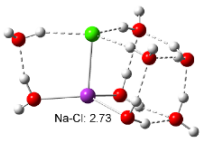

0.000

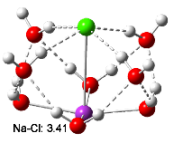

0.061

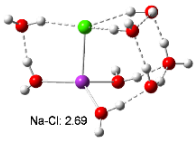

0.112

0.117

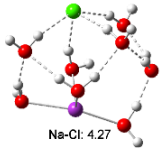

0.118

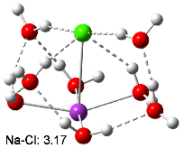

0.125

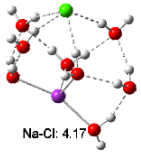

0.128

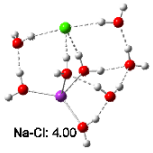

0.129

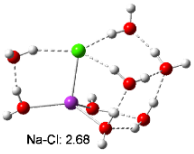

0.132

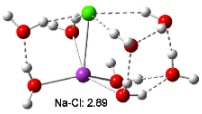

0.137

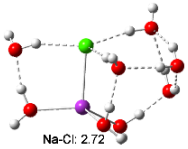

0.153

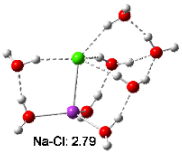

0.153

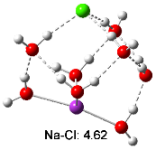

0.155

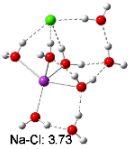

0.156

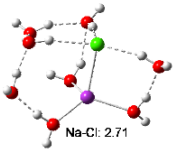

0.158

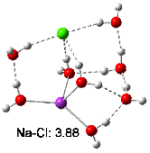

0.161

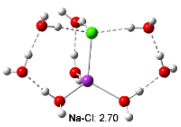

0.162

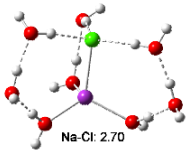

0.164

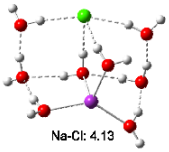

0.167

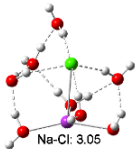

0.167

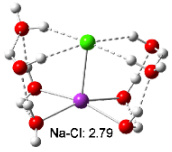

0.170

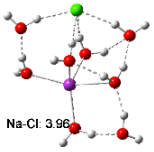

0.172

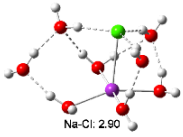

0.180

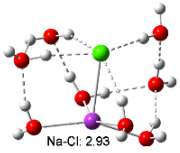

0.180

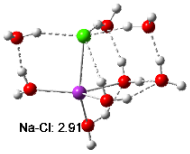

0.182

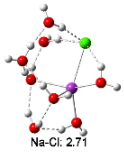

0.189

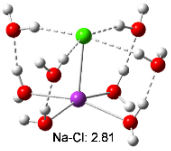

0.190

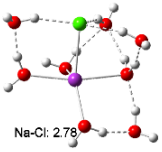

0.192

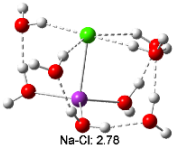

0.196

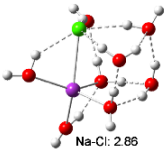

0.196

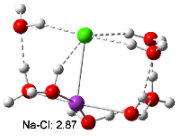

0.197

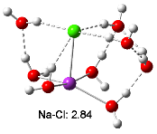

0.197

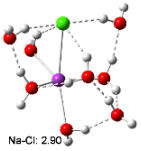

0.198

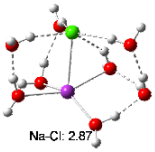

0.200

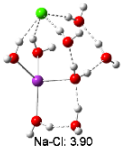

0.206

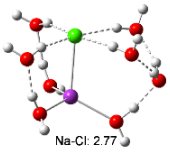

0.207

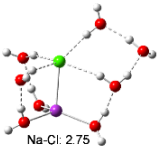

0.209

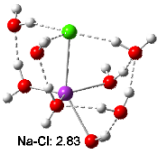

0.213

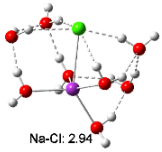

0.216

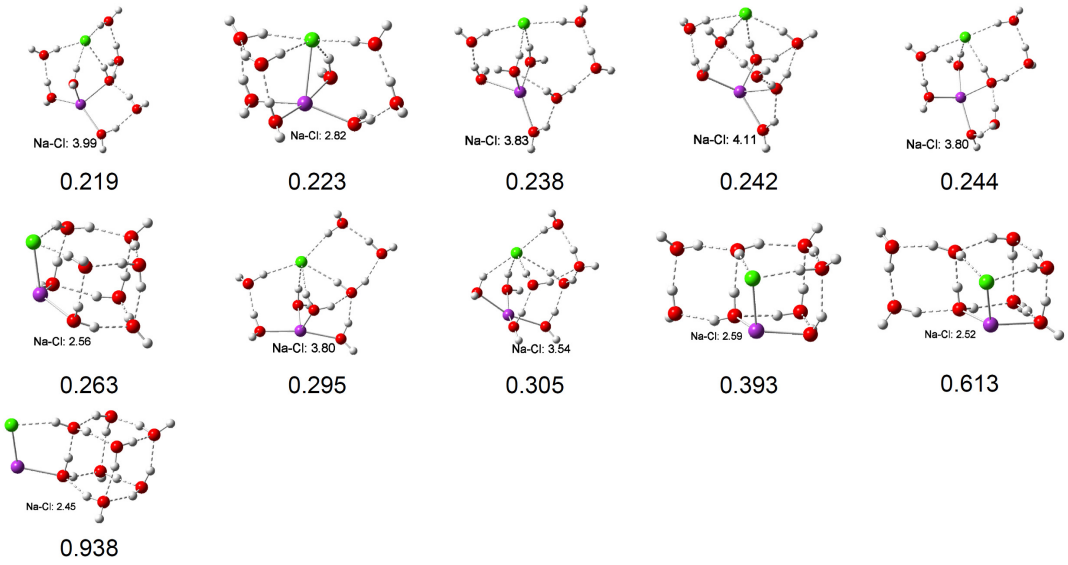

Figure S8. Complete list of optimized isomers of $NaCl(H_2O)_8$ at LC-ωPBE/6-311++G(d,p) level. Those reported in the main text are highlighted in green. Relative energies (in eV using LC-ωPBE functional within ZPE correction) and Na–Cl distances (in Å) are indicated.

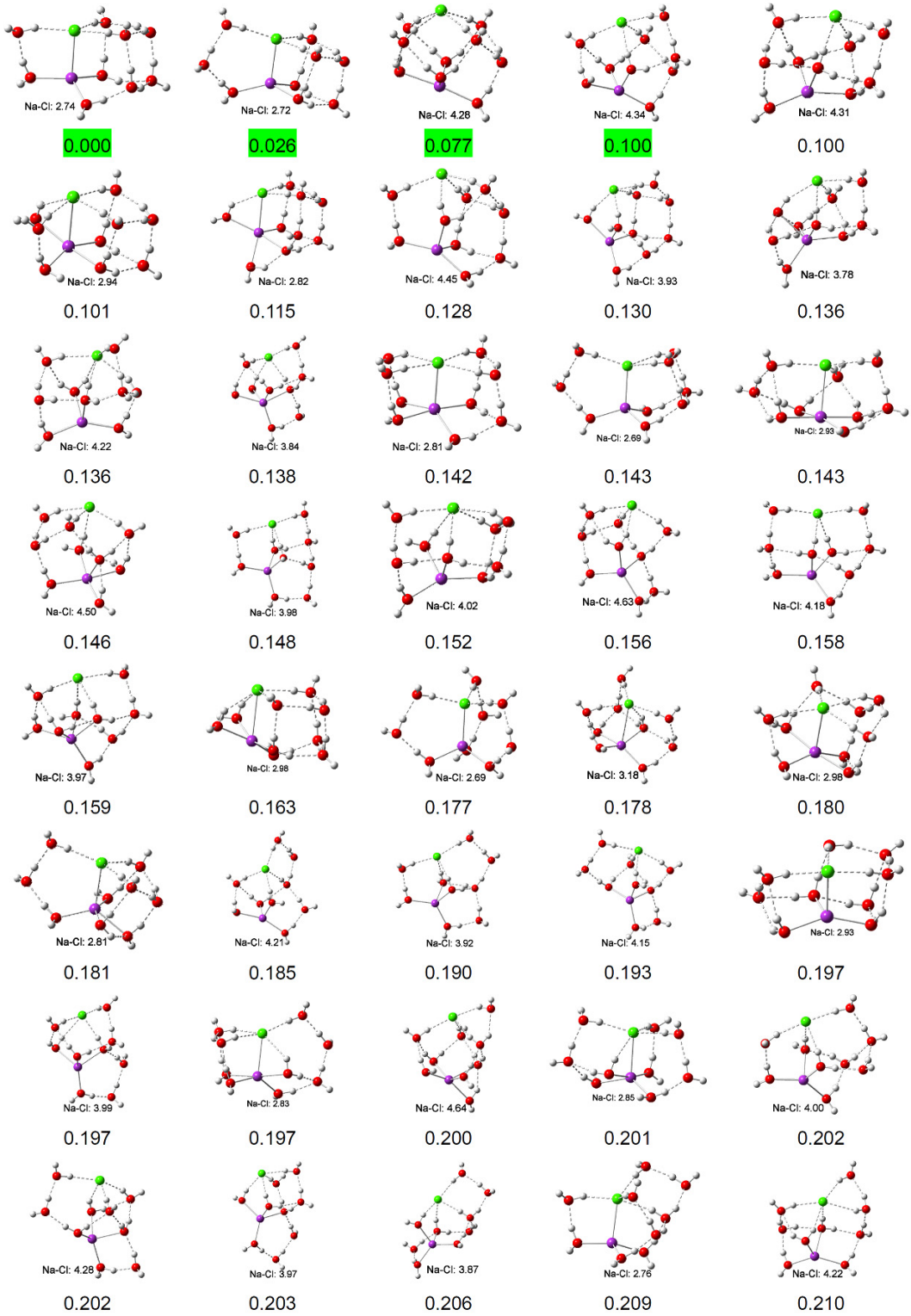
Na-Cl: 2.74
0.000
Na-Cl: 2.72
0.026
Na-Cl: 4.28
0.077
Na-Cl: 4.34
0.100
Na-Cl: 4.31
0.100
Na-Cl: 2.94
0.101
Na-Cl: 2.82
0.115
Na-Cl: 4.45
0.128
Na-Cl: 3.93
0.130
Na-Cl: 3.78
0.136
Na-Cl: 4.22
0.136
Na-Cl: 3.84
0.138
Na-Cl: 2.81
0.142
Na-Cl: 2.69
0.143
Na-Cl: 2.93
0.143
Na-Cl: 4.50
0.146
Na-Cl: 3.98
0.148
Na-Cl: 4.02
0.152
Na-Cl: 4.63
0.156
Na-Cl: 4.18
0.158
Na-Cl: 3.97
0.159
Na-Cl: 2.98
0.163
Na-Cl: 2.69
0.177
Na-Cl: 3.18
0.178
Na-Cl: 2.98
0.180
Na-Cl: 2.81
0.181
Na-Cl: 4.21
0.185
Na-Cl: 3.92
0.190
Na-Cl: 4.15
0.193
Na-Cl: 2.93
0.197
Na-Cl: 3.99
0.197
Na-Cl: 2.83
0.197
Na-Cl: 4.64
0.200
Na-Cl: 2.85
0.201
Na-Cl: 4.00
0.202
Na-Cl: 4.28
0.202
Na-Cl: 3.97
0.203
Na-Cl: 3.87
0.206
Na-Cl: 2.76
0.209
Na-Cl: 4.22
0.210

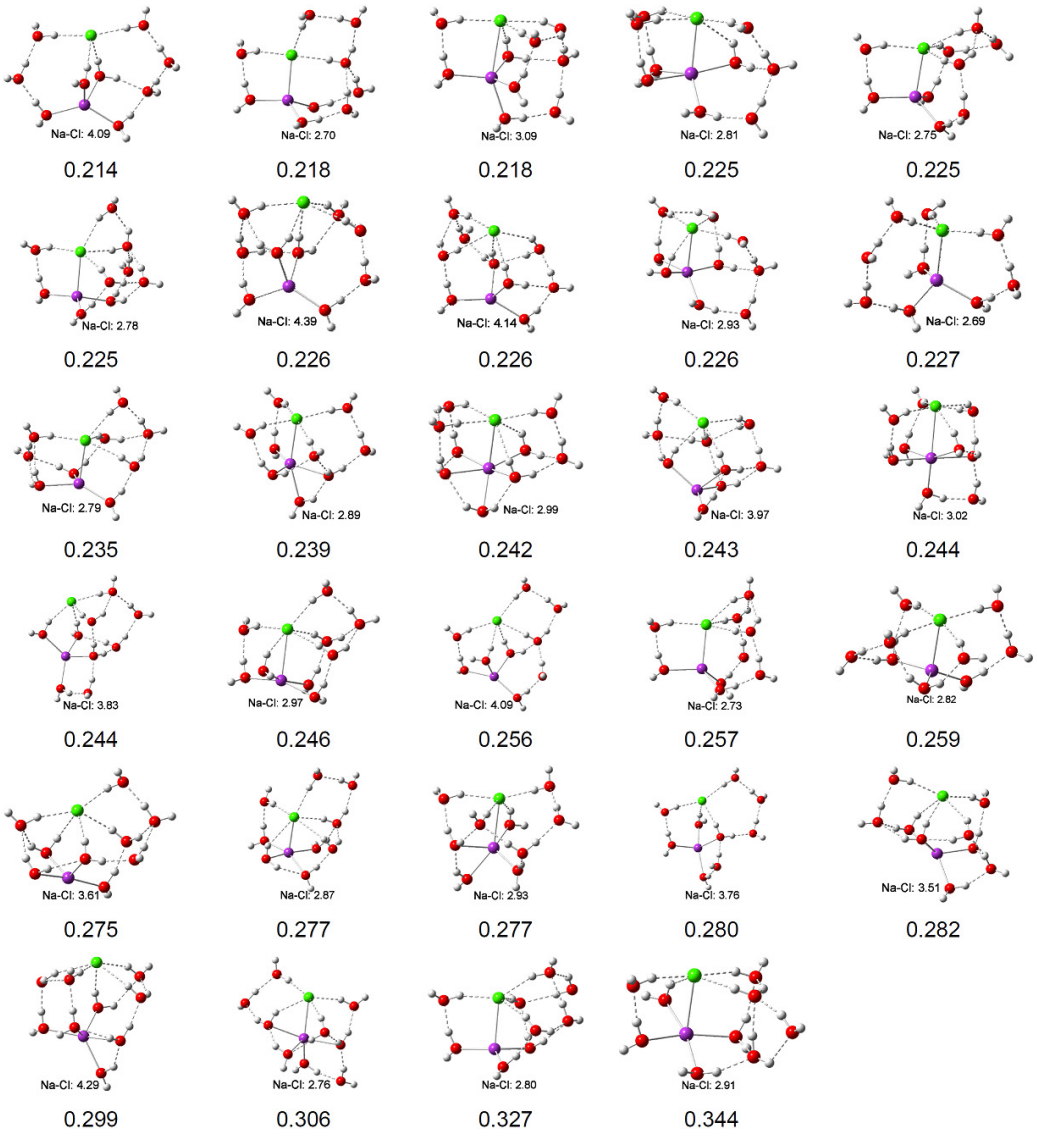

Figure S9. Complete list of optimized isomers of $NaCl(H_2O)_9$ at LC-ωPBE/6-311++G(d,p) level. Those reported in the main text are highlighted in green. Relative energies (in eV using LC-ωPBE functional within ZPE correction) and Na–Cl distances (in Å) are indicated.

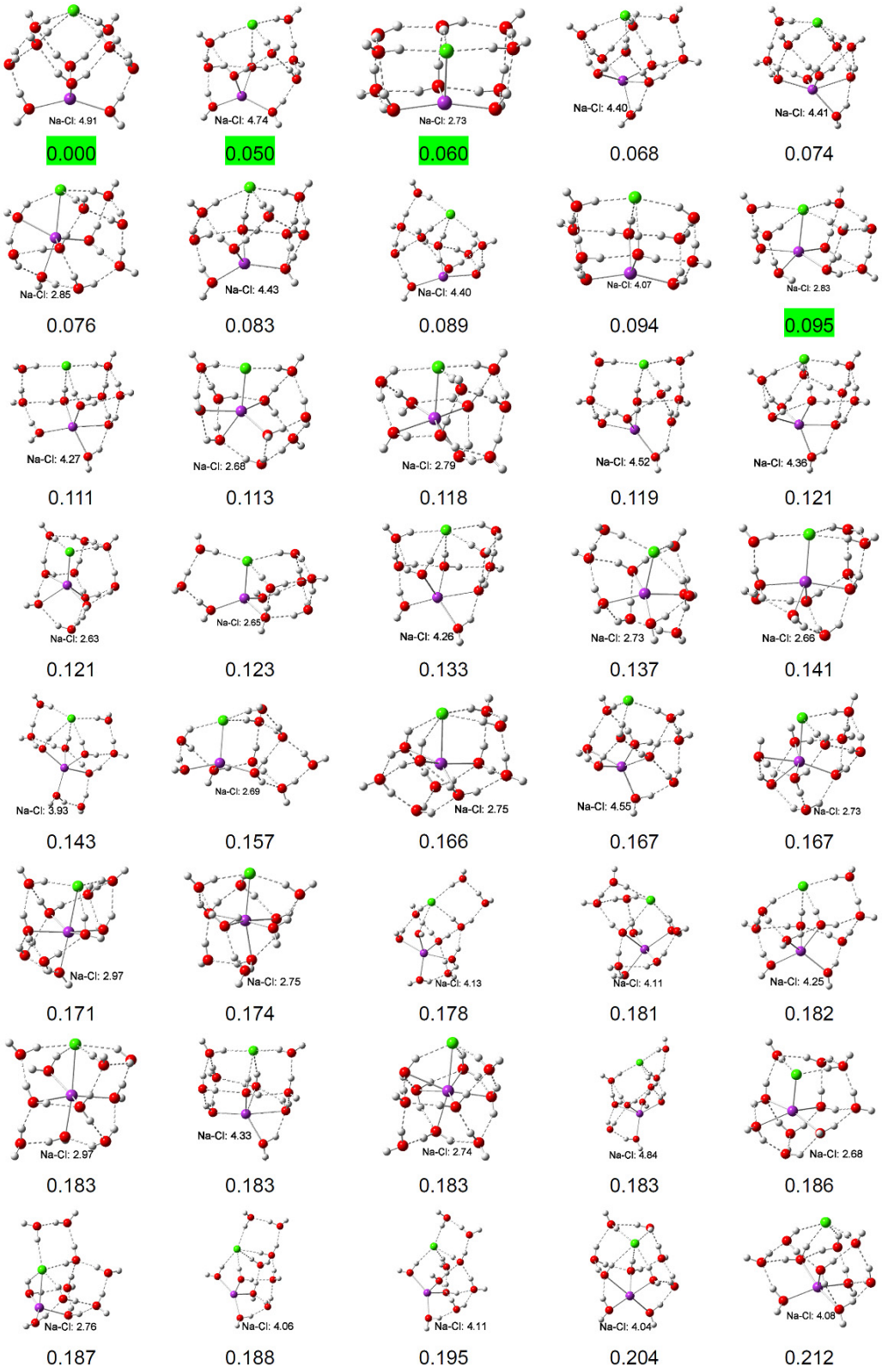
Na-Cl: 4.91
0.000
Na-Cl: 4.74
0.050
Na-Cl: 2.73
0.060
Na-Cl: 4.40
0.068
Na-Cl: 4.41
0.074
Na-Cl: 2.85
0.076
Na-Cl: 4.43
0.083
Na-Cl: 4.40
0.089
Na-Cl: 4.07
0.094
Na-Cl: 2.83
0.095
Na-Cl: 4.27
0.111
Na-Cl: 2.68
0.113
Na-Cl: 2.79
0.118
Na-Cl: 4.52
0.119
Na-Cl: 4.36
0.121
Na-Cl: 2.63
0.121
Na-Cl: 2.65
0.123
Na-Cl: 4.26
0.133
Na-Cl: 2.73
0.137
Na-Cl: 2.66
0.141
Na-Cl: 3.93
0.143
Na-Cl: 2.69
0.157
Na-Cl: 2.75
0.166
Na-Cl: 4.55
0.167
Na-Cl: 2.73
0.167
Na-Cl: 2.97
0.171
Na-Cl: 2.75
0.174
Na-Cl: 4.13
0.178
Na-Cl: 4.11
0.181
Na-Cl: 4.25
0.182
Na-Cl: 2.97
0.183
Na-Cl: 4.33
0.183
Na-Cl: 2.74
0.183
Na-Cl: 4.84
0.183
Na-Cl: 2.68
0.186
Na-Cl: 2.76
0.187
Na-Cl: 4.06
0.188
Na-Cl: 4.11
0.195
Na-Cl: 4.04
0.204
Na-Cl: 4.08
0.212

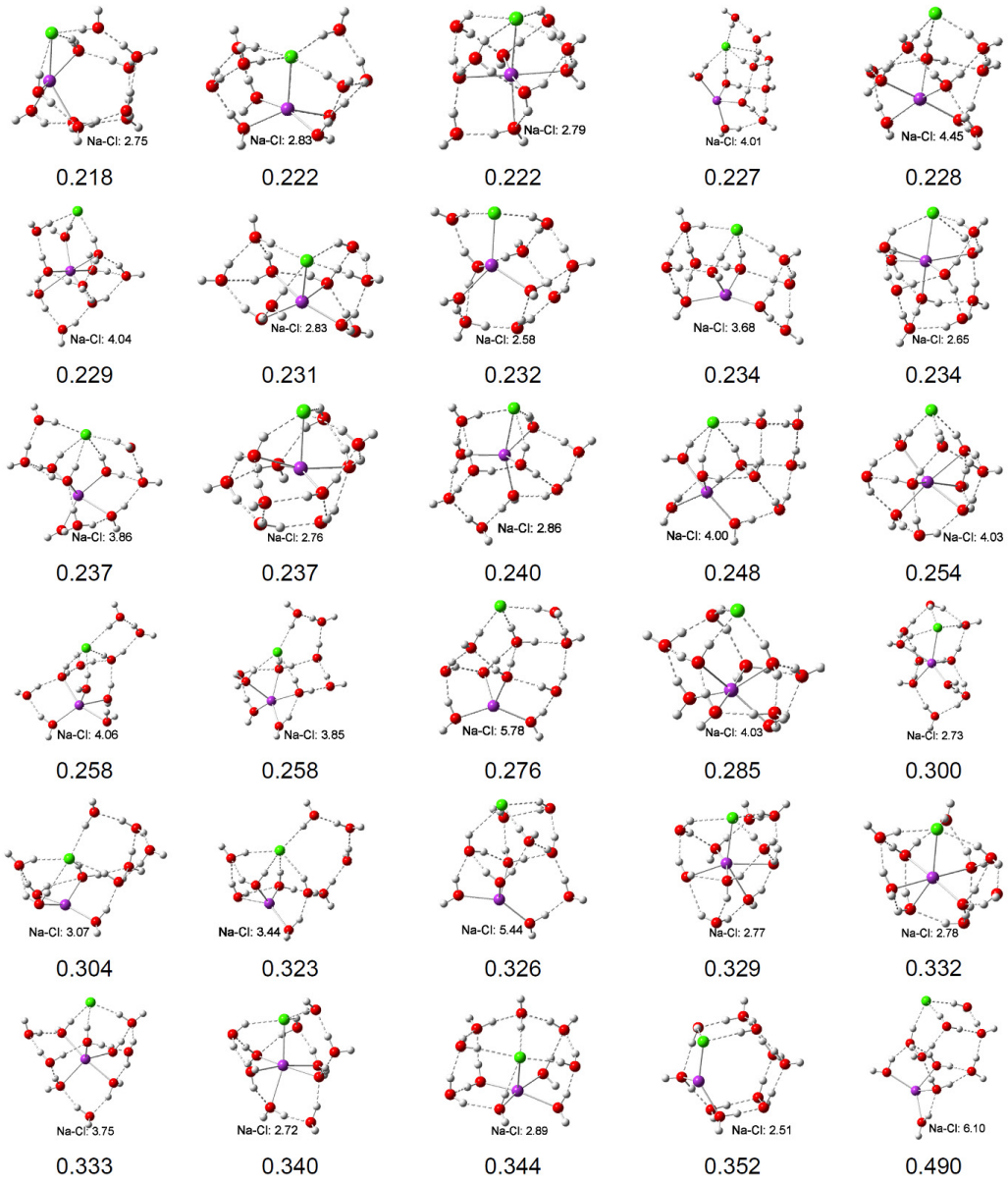

Figure S10. Complete list of optimized isomers of $NaCl(H_2O)_{10}$ at LC-ωPBE/6-311++G(d,p) level. Those reported in the main text are highlighted in green. Relative energies (in eV using LC-ωPBE functional within ZPE correction) and Na–Cl distances (in Å) are indicated.

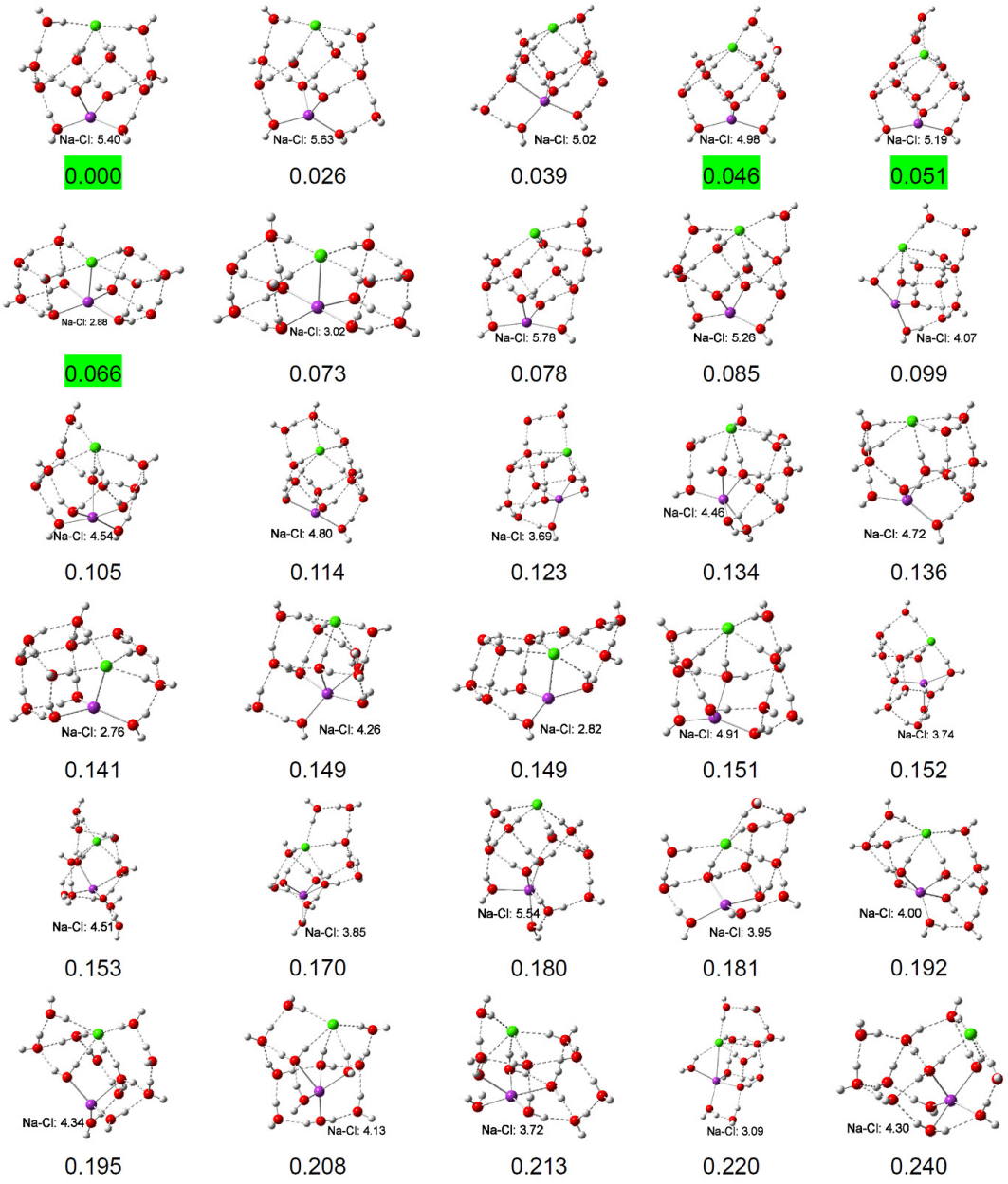

Figure S11. Complete list of optimized isomers of $NaCl(H_2O)_{12}$ at LC-ωPBE/6-311++G(d,p) level. Those reported in the main text are highlighted in green. Relative energies (in eV using LC-ωPBE functional within ZPE correction) and Na–Cl distances (in Å) are indicated.

References

S1. Xu, H.-G.; Zhang, Z.-G.; Feng, Y.; Yuan, J. Y.; Zhao, Y. C.; Zheng, W. J. Vanadium-doped small silicon clusters: photoelectron spectroscopy and density-functional calculations. *Chem. Phys. Lett.* **2010,** *487*, 204-208.

S2. Gao, Y. Q. Self-adaptive enhanced sampling in the energy and trajectory spaces: accelerated thermodynamics and kinetic calculations. *J. Chem. Phys.* **2008,** *128*, 134111.

S3. Vydrov, O. A.; Scuseria, G. E. Assessment of a long-range corrected hybrid functional. *J. Chem. Phys.* **2006,** *125*, 234109.

S4. Frisch, M. J.; Trucks, G. W.; Schlegel, H. B.; Scuseria, G. E.; Robb, M. A.; Cheeseman, J. R.; Scalmani, G.; Barone, V.; Mennucci, B.; Petersson, G. A.; Nakatsuji, H.; Caricato, M.; Li, X.; Hratchian, H. P.; Izmaylov, A. F.; Bloino, J.; Zheng, G.; Sonnenberg, J. L.; Hada, M.; Ehara, M.; Toyota, K.; Fukuda, R.; Hasegawa, J.; Ishida, M.; Nakajima, T.; Honda, Y.; Kitao, O.; Nakai, H.; Vreven, T.; Montgomery, J. A., Jr.; Peralta, J. E.; Ogliaro, F.; Bearpark, M.; Heyd, J. J.; Brothers, E.; Kudin, K. N.; Staroverov, V. N.; Kobayashi, R.; Normand, J.; Raghavachari, K.; Rendell, A.; Burant, J. C.; Iyengar, S. S.; Tomasi, J.; Cossi, M.; Rega, N.; Millam, J. M.; Klene, M.; Knox, J. E.; Cross, J. B.; Bakken, V.; Adamo, C.; Jaramillo, J.; Gomperts, R.; Stratmann, R. E.; Yazyev, O.; Austin, A. J.; Cammi, R.; Pomelli, C.; Ochterski, J. W.; Martin, R. L.; Morokuma, K.; Zakrzewski, V. G.; Voth, G. A.; Salvador, P.; Dannenberg, J. J.; Dapprich, S.; Daniels, A. D.; Farkas, Ö.; Foresman, J. B.; Ortiz, J. V.; Cioslowski, J.; Fox, D. J. Gaussian 09, Revision **A.01**, Gaussian, Inc., Wallingford CT, 2009.

S5. Krishnan, R.; Binkley, J. S.; Seeger, R.; Pople, J. A. Self-consistent molecular orbital methods. XX. a basis set for correlated wave functions. *J. Chem. Phys.* **1980,** *72*, 650-654.

S6. Pople, J. A.; Head-Gordon, M.; Raghavachari, K. Quadratic configuration interaction: a general technique for determining electron correlation energies. *J. Chem. Phys.* **1987,** *87*, 5968-5975.

S7. Head-Gordon, M.; Pople, J. A.; Frisch, M. J. MP2 energy evaluation by direct methods. *Chem. Phys. Lett.* **1988,** *153*, 503-506.

S8. Dunning, T. H., Jr. Gaussian basis sets for use in correlated molecular calculations. I. the atoms boron through neon and hydrogen. *J. Chem. Phys.* **1989,** *90*, 1007-1023.

S9. Woon, D. E.; Dunning, T. H., Jr. Gaussian basis sets for use in correlated molecular calculations. III. the atoms aluminum through argon. *J. Chem. Phys.* **1993,** *98*, 1358-1371.

S10. Papajak, E.; Leverentz, H. R.; Zheng, J.; Truhlar, D. G. Efficient diffuse basis sets: cc-pVxZ+ and maug-cc-pVxZ. *J. Chem. Theory Comput.* **2009,** *5*, 1197-1202.

S11. Gao, Y. Q. An integrate-over-temperature approach for enhanced sampling. *J. Chem. Phys.* **2008**, *128*, 064105.

S12. Berendsen, H. J. C.; Grigera, J. R.; Straatsma, T. P. The missing term in effective pair potentials. *J. Chem. Phys.* **1987**, *91*, 6269-6271.

S13. Joung, I. S.; Cheatham, T. E. determination of alkali and halide monovalent ion parameters for use in explicitly solvated biomolecular simulations. *J. Phys. Chem. B* **2008**, *112*, 9020-9041.

S14. Wu, X. W.; Brooks, B. R. Self-guided langevin dynamics simulation method. *Chem. Phys. Lett.* **2003**, *381*, 512-518.

S15. Case, D. A. D., T. A.; Cheatham; Simmerling, C. L.; Wang, J.; Duke, R. E.; Luo, R.; Merz, K. M.; Pearlman, D. A.; Crowley, M.; Walker, R. C.; Zhang, W.; Wang, B.; Hayik, S.; Roitberg, A.; Seabra,

G.; Wong, K. F.; Paesani, F.; Wu, X.; Brozell, S.; Tsui, V.; Gohlke, H.; Yang, L.; Tan, C.; Mongan, J.; Hornak, V.; Cui, G.; Beroza, P.; Mathews, D. H.; Schafmeister, C.; Ross, W. S.; Kollman, P. A., Amber 9. 2006.

S16. Yang, L.; Shao, Q.; Gao, Y. Q. Thermodynamics and folding pathways of Trpzip2: an accelerated molecular dynamics simulation study. *J. Phys. Chem. B* **2008**, *113*, 803-808.